Molecular, structural and optical properties of S-alanine S-mandelic acid crystals

K. Sivakumar[1], M. Senthilkumar[2] and C. Ramachandra raja[3]*

[1, 2, 3]Department of Physics, Government Arts College (Autonomous), Kumbakonam- 612 002, India.
*Corresponding author: Tel: +91-9976696277.
E-mail address: crrajaphy@gmail.com, crraja_phy@yahoo.com.

Abstract

S-alanine S-mandelic acid (SASM) single crystals were grown by solvent evaporation procedure. They were characterized by single crystal and powder XRD analysis to determine the lattice constants. The good optical transparency of SMSA crystal was confirmed by UV-Vis-NIR spectroscopy and the cut-off wavelength is 278 nm. The vibrations of functional groups were determined using FT-IR and FT-Raman spectroscopy. The molecular structure of the grown crystal was established by ^{13}C-NMR spectroscopy. The nonlinear optical property of the crystal was confirmed by SHG technique. Nonlinear refractive index (n_2), nonlinear absorption coefficient (β) and third order nonlinear susceptibility (χ^3) were evaluated by Z-scan technique. The third order nonlinear optical susceptibility ($\chi3$) of SASM crystal is better than other NLO single crystals.

Keywords

Crystal growth; XRD; Spectroscopy; NMR; Nonlinear optics; Z- scan

1. Introduction

Nonlinear optical crystals are used to generate laser radiation at new frequencies with the help of several NLO processes such as second harmonic generation, third harmonic generation, sum frequency generation, difference frequency generation and optical parametric oscillation. These crystals are classified into three type's namely organic, inorganic and semiorganic crystals. Organic NLO crystals exhibit higher SHG efficiency when compared to the other two types. Further several structural designs are possible in these crystals [1-4].

In the family of organic materials, amino acids are considered to be interesting materials for NLO devices as they contain proton donor carboxylic (COOH) group and the proton acceptor amino (NH_2) group. Several amino acid based crystals were grown and characterized for device applications [5–7].

Among the amino acids, S-alanine (CH_3CHNH_2COOH) is the smallest and simplest molecule having SHG efficiency of about one third of that of the well known potassium dihydrogen phosphate (KDP). Cobalt chloride doped S-alanine has SHG efficiency of 0.74 time that of KDP [8]. In the present work S-mandelic acid was added with S-alanine and crystals of SASM were grown. The SHG efficiency is found to be increased in this material.

The structure of SASM was reported by Zi-Quang Hu et al [9]. The properties of the crystal are not reported so far. Hence, the grown crystals were characterized by single crystal and powder XRD analysis, UV-Vis-NIR spectroscopy, FT-IR and FT-Raman spectroscopy, ^{13}C- NMR spectroscopy, SHG test, Z-scan test and the results are reported.

2. Experimental

2.1. Synthesis for SASM crystal

Single crystals of SASM were grown by reacting SA and SMA taken in the molar ratio 1:1 respectively dissolving the mixture in deionized water in a beaker, stirred good in a magnetic stirrer. This solution was filtered and this filtered solution was maintained at 37° C using a constant temperature bath with an accuracy of ± 0.1°C. Due to slow evaporation of the solvent the solution become supersaturated. Transparent single crystals of SASM were grown at the bottom of the beaker in a period of 25 days.

3. Result and Discussion

3.1. Single crystal XRD analysis

This analysis reveals that SASM crystallizes in monoclinic system with non centrosymmetric space group C2. The measured lattice constants are a= 17.76 ± 0.07 Å, b=5.39 ± 0.01 Å, c=12.41 ± 0.05 Å, α = γ= 90, β =100.67 ± 0.07 ° and the cell volume (V) = 1166 ± 13 Å^3. These results are in good agreement with the values reported in literature [9].

3.2. Powder XRD analysis

The powder XRD pattern of SASM is shown in Fig. 1. The sample was scanned for 2θ values from 5°–80º at the rate of 1º/ min. By using the lattice parameters values taken from single crystal XRD, powder XRD diffraction peaks of the crystal have been indexed using the software package Indx. And using the simulated hkl and d spacing values, lattice parameters are calculated with the programme, Unitcell. The calculated lattice parameters are compared with the lattice parameters obtained from single crystal XRD and presented in Table 1. It shows that the lattice parameters calculated from powder XRD is closely matched with results obtained from single crystal XRD.
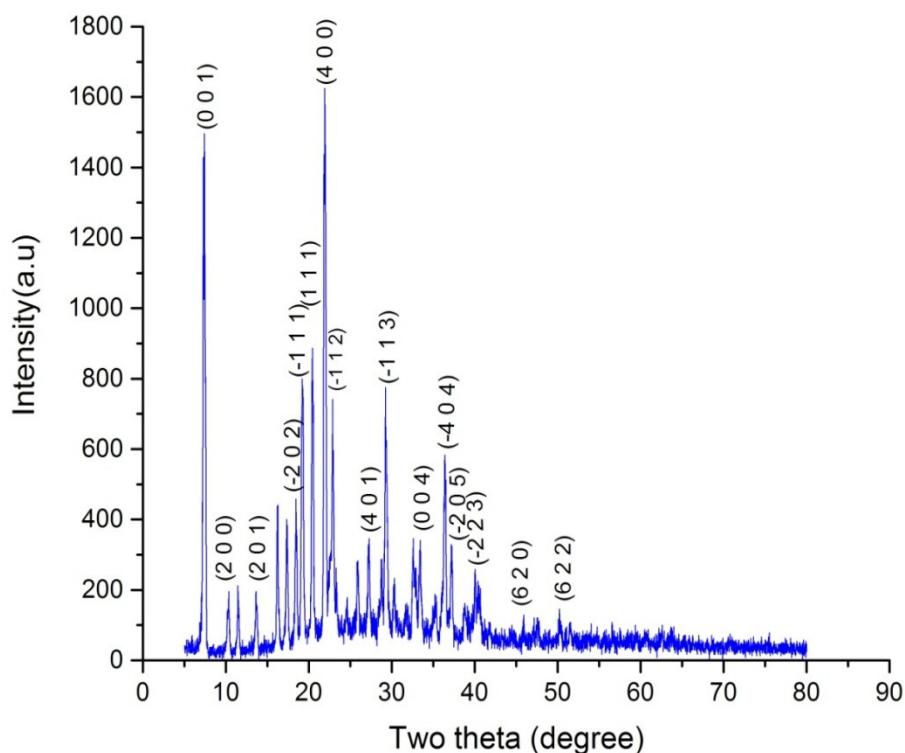

Fig.1. Powder XRD pattern of SASM crystal

Table 1: Comparison of crystal data

Lattice parameters	a (Å)	b (Å)	c (Å)	β (°)	V(Å)³
Single crystal XRD	17.76 ± 0.07	5.39 ± 0.01	12.41 ± 0.05	100.67 ± 0.07	1166 ± 13
Powder XRD	17.65	5.41	12.40	100.55	1166
Reported value [9]	17.795	5.394	12.431	100.650	1172.7

3.3. UV-Vis-NIR Analysis

The percentage of transmittance vs. wavelength of SASM crystal is shown in **Fig. 2.** The thickness of the crystal used in this study is 2 mm. From this measurement, it is observed that the crystal is transparent in the wavelength range of 278–1100 nm. The UV transparency cut-off wavelength of SASM single crystal occurs at 278 nm. This transmission window is sufficient for the generation of second and third harmonic of Nd: YAG laser (1064 nm) or other applications in the visible region. This suggests that the crystal can be used effectively in converting the Nd:YAG fundamental wavelength, 1064 nm, into its second harmonic, 532 nm and third harmonic, 355 nm.
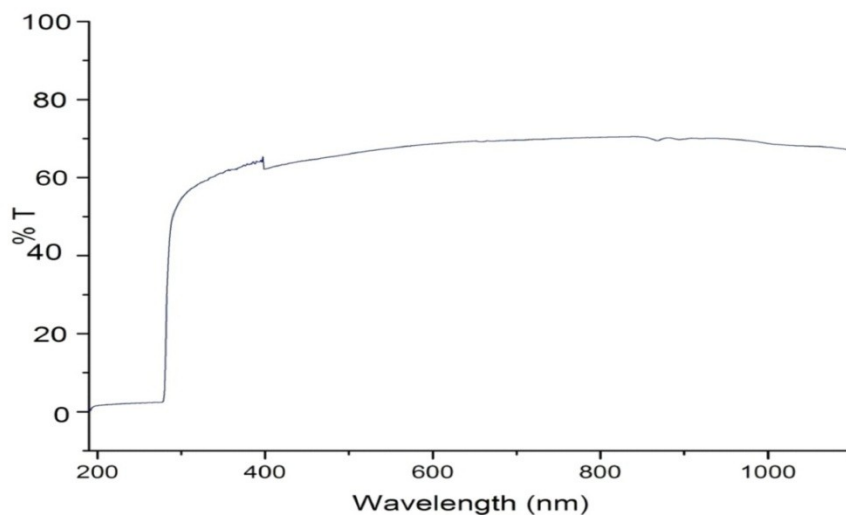
Fig. 2 UV–Vis–NIR spectrum of SASM crystal

3.4. FT-IR and FT-Raman spectral study of SASM

The FT-IR and FT-Raman spectra of SASM single crystal in shown in Fig. 3 and Fig. 4 respectively. The peak observed at 3095 cm^{-1} in FT-IR corresponds to NH_3^+ symmetric stretching and the same is observed at 3065 cm^{-1} in FT-Raman spectrum. The peak observed at 3017 cm^{-1} in FT-IR corresponds to NH_3^+ asymmetric stretching and the same is observed at 2997 cm^{-1} in FT-Raman spectrum. In the FT-Raman spectrum the peak observed at 2740 cm^{-1} corresponds to C-H stretching and it is observed at 2747 cm^{-1} in FT-IR spectrum. The peak observed at 1599 cm^{-1} in FT-IR corresponds to C=O stretching and the same is observed at 1601 cm^{-1} in FT-Raman spectrum. The peaks are assigned FT-IR at 1494 cm^{-1}, 1402 cm^{-1} is attributed to COO$^-$ stretching and the same is observed at 1497 cm^{-1}, 1423 cm^{-1} in FT-Raman spectrum. The peak at 1458 cm^{-1} in FT-IR and the one at 1459 cm^{-1} in FT-Raman are assigned to CH vibration. The peak observed at 1357 cm^{-1} in FT-IR corresponds to C-N vibration and the same is observed at 1352 cm^{-1} in FT-Raman spectrum. The peak observed at 1310 cm^{-1} in FT-IR corresponds to COO$^-$ stretching and the same is observed at 1298 cm^{-1} in FT-Raman spectrum. The peak at 1216 cm^{-1} and 1182 cm^{-1} in FT-IR and FT-Raman respectively corresponds to C-O stretching. The peaks at 1151 cm^{-1}, 1116 cm^{-1} in FT-IR and corresponding peaks observed at 1154 cm^{-1} and 1113 cm^{-1} in FT-Raman corresponds to COO$^-$ stretching. The peak observed at 1056 cm^{-1} in FT-IR corresponds to C-C vibration and the same is observed at 1028 cm^{-1} in FT-Raman spectrum. In FT-IR, peak at 982 cm^{-1} and the same at 1003 cm^{-1} in FT-Raman corresponds to C-N stretching. The FT-IR and FT-Raman peaks observed at 888 cm^{-1} and 863 cm^{-1} respectively corresponds to C-C-N stretching. The FT-IR and FT-Raman peaks observed at 827 cm^{-1} and 795 cm^{-1} respectively corresponds to C-H stretching. The peak at 731 cm^{-1} in FT-IR is corresponds to C-H rocking and the same is observed at 747 cm^{-1} in FT-Raman spectrum. The FT-IR and FT-Raman peaks observed at 628 cm^{-1} and 618 cm^{-1} respectively corresponds to COOH bending. The peak at 501 cm^{-1} in FT-IR is corresponds to OH rocking and the same is observed at 511 cm^{-1} in FT-Raman spectrum [10-12]. The presence of vibrational bands both in IR and Raman spectra establishes the noncentrosymmetric nature of the SASM molecule. All the vibrational bands assigned in IR and Raman spectra have been listed in Table 2.

Table 2: FT-IR and FT-Raman assignments of SASM crystal

FT-IR (cm^{-1})	FT-Raman (cm^{-1})	Assignments
3095	3065	NH_3^+ symmetric stretching
3017	2997	NH_3^+ asymmetric stretching
2747	2740	C-H stretching
1599	1601	C=O stretching
1494,1402	1497,1423	COO$^-$ stretching
1458	1459	CH vibration
1357	1352	C-N vibration
1310	1298	COO$^-$ stretching
1216	1182	C-O stretching
1151, 1116	1154, 1113	COO$^-$ stretching

International Journal of Research

Available at https://edupediapublications.org/journals

e-ISSN: 2348-6848
p-ISSN: 2348-795X
Volume 05 Issue-01
January 2018

1056	1028	C-C stretching
982	1003	C-N stretching
888	863	C-C-N stretching
827	795	C-H stretching
731	747	C-H rocking
628	618	COOH bending
501	511	OH rocking
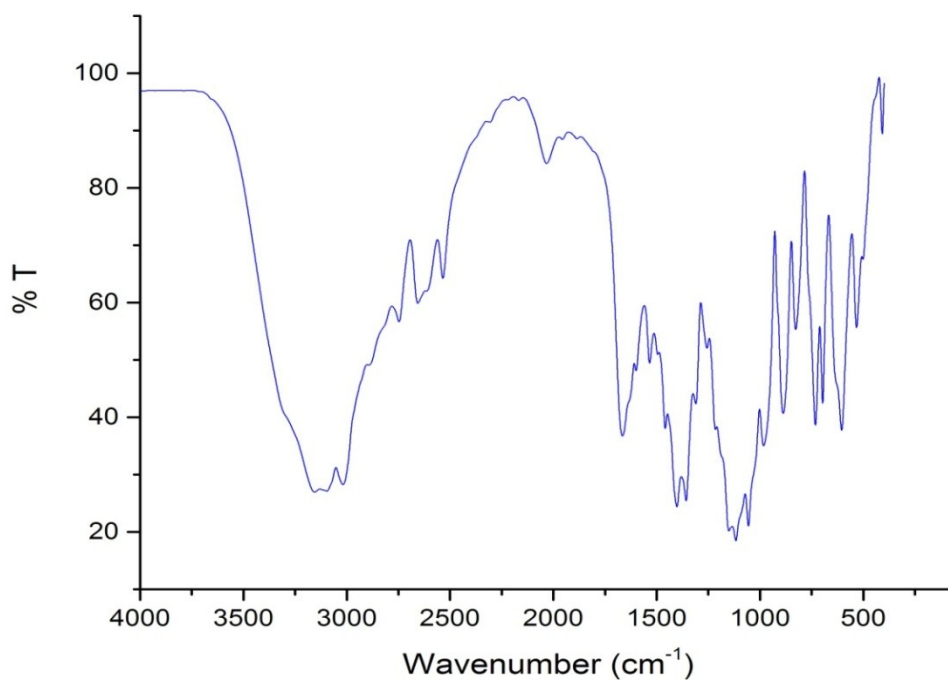
Fig.3. FT-IR spectrum of SASM crystal
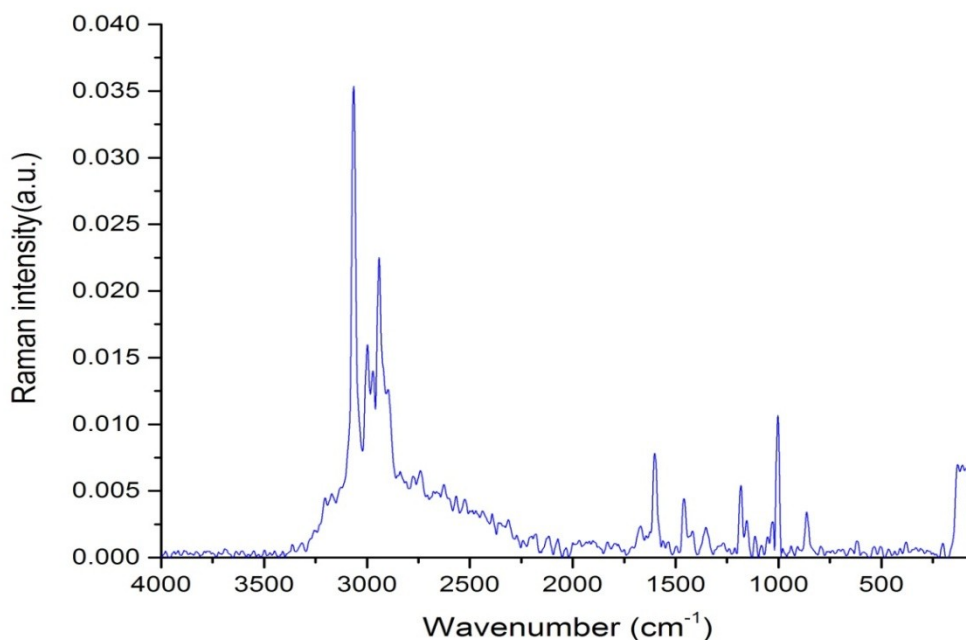
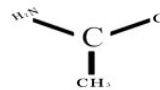**Fig.4. FT-Raman spectrum of SASM crystal**

3.5 NMR analysis

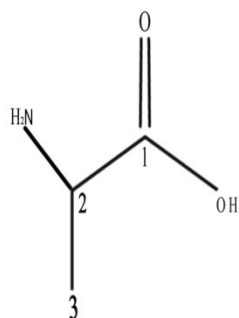The ^{13}C-NMR spectrum of SASM crystal is presented in Fig. 6. The chemical shifts are tabulated with assignments in Table 3. The ^{13}C-NMR spectrum of SASM can be understood with the help of the molecular structure shown in Fig.5 [13].

The signal observed at 176.90 ppm corresponds to the carbon 1 (COOH group of S-alanine). The signal observed at 174.87 ppm corresponds to the carbon 1 (COOH group of S-mandelic acid). The signal at 138.49 ppm is due to carbon 2 (⎯C⎯ group of S-mandelic acid). The signals observed at 128.96 ppm, 128.79 ppm and 127.02 ppm were due to carbon 3, 4 and 5
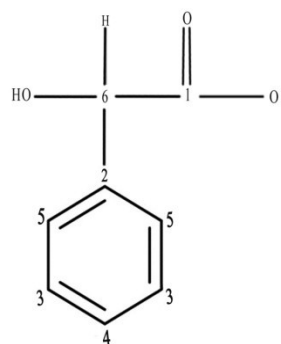
(CH group of S-mandelic acid). The signal observed at 73.29 ppm is due to carbon 6 (⎯C⎯ group of S-mandelic acid). The signal at 49.94 ppm is due to carbon 2 (group of S-alanine). The signal at 15.81 ppm is due to carbon 3 (CH$_3$ group of S-alanine). The signals observed for all the carbon atoms of S-alanine and S-mandelic acid establishes the formation of SASM molecule. The results are in agreement with the reported values [13].

International Journal of Research

Available at https://edupediapublications.org/journals

e-ISSN: 2348-6848
p-ISSN: 2348-795X
Volume 05 Issue-01
January 2018

S-alanine

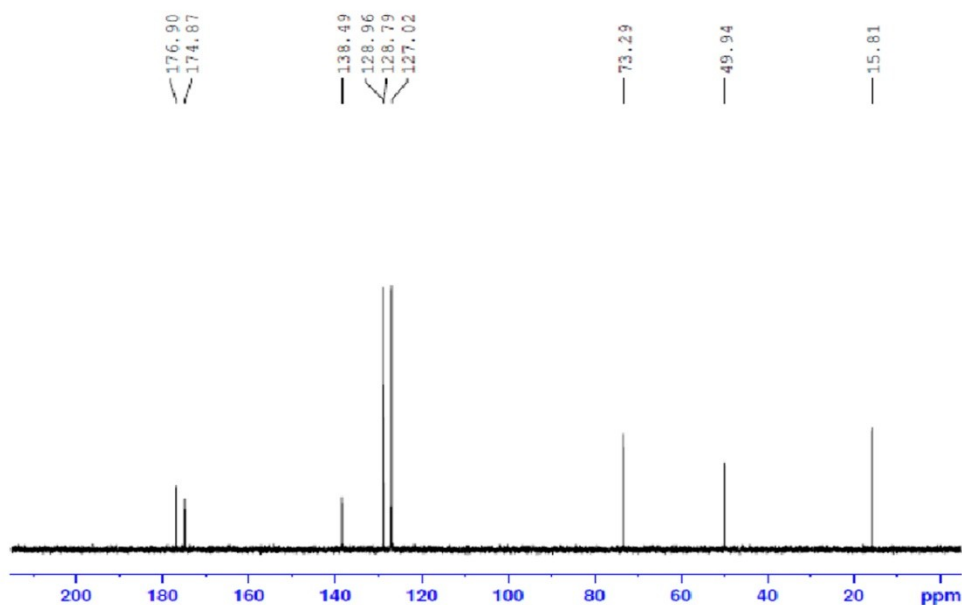S-mandelic acid

Fig.5 ^{13}C-NMR atomic numbering of SASM crystal

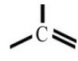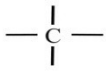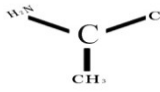**Fig.6 ^{13}C-NMR spectrum of SASM crystal**

Table 3: Chemical shifts in ^{13}C-NMR spectrum of SASM

Chemical shift (ppm)	Group identification
176.90	Carbon 1 (COOH group of S-alanine).
174.87	Carbon 1 (COOH group of S-mandelic acid)
138.49	Carbon 2 (group of S-mandelic acid)
128.96	Carbon 3 (CH group of S-mandelic acid)
128.79	Carbon 4 (CH group of S- mandelic acid)
127.02	Carbon 5 (CH group of S-mandelic acid)
73.29	Carbon 6 (group of S-mandelic acid)
49.94	Carbon 2 (group of S- alanine)

15.81	Carbon 3 (CH$_3$ group of S- alanine)

3.6. Second Harmonic Generation Analysis

The Kurtz and Perry method was employed to measure powder SHG efficiency of SASM single crystals. The grown crystals grind into very fine powder and tightly packed in a micro capillary tube which served as the sample cell. Then it was mounted in the path of Nd:YAG laser with first harmonic output of 1064 nm with the pulse width of 6 ns. The input beam energy of 1.2 mJ/ pulse is used. Potassium dihydrogen phosphate (KDP) is used as the reference material. The emission of green light of wavelength 532 nm from SASM crystal confirms the SHG property. The SHG output (532 nm) is finally detected by a photomultiplier tube and displayed on the oscilloscope. The measured output power was found to be 20 mV and 22 mV for SASM and KDP, respectively. The SHG efficiency of SASM was found to be 0.91 times that of KDP. The second harmonic generation efficiency of a material depends on its molecular structure. In SASM, each S-alanine molecule is hydrogen bonded to three S-mandelic acid molecules and vice versa. There is a strong H-bonding between the carboxylate (COO$^-$ group) of alanine and the carboxyl (COOH group) of S-mandelic acid. The charge transfer across the bonding groups determines the second harmonic generation output. The presence of these hydrogen bonds are responsible for the SHG efficiency [9]. SHG efficiency of some amino acid based crystals are compared in Table 4.

Table 4: SHG efficiency of some amino acid based crystals

Crystal	SHG efficiency	Reference
L-alanine	0.33	14
L-alanine cadmium hydrobromide	0.5	12
L-alanine strontium chloride trihydrate	0.7	15
Cobalt chloride doped L-alanine	0.74	8
L-alanine cadmium chloride	0.87	16

SASM	0.91	**Present work**

3.7. Z-scan Measurement

The *Z*-scan technique is a simple and effective tool for determining the nonlinear properties. Figure 7 and Figure 8 show the open and closed aperture Z-scan curve for the SASM crystal.

The peak followed by the valley in the closed aperture curve is due to a negative refractive index ($n_2 = 1.2 \times 10^{-12}$ cm^2/W) of the material and it results in defocusing nature of the material, which is an essential property for the application in the protection of optical sensors such as night vision devices [17].

In the open aperture curve, maximum transmission occurs near the focus. This is due to saturable absorption of the material. Saturable absorption nature of the crystal suggests that it can be used as a passive Q-switch in pulsed laser systems [18].

The third order nonlinear optical susceptibility (χ3) of SASM crystal is better than some of the reported crystals (Table 5).

Table 5: Comparison of χ3

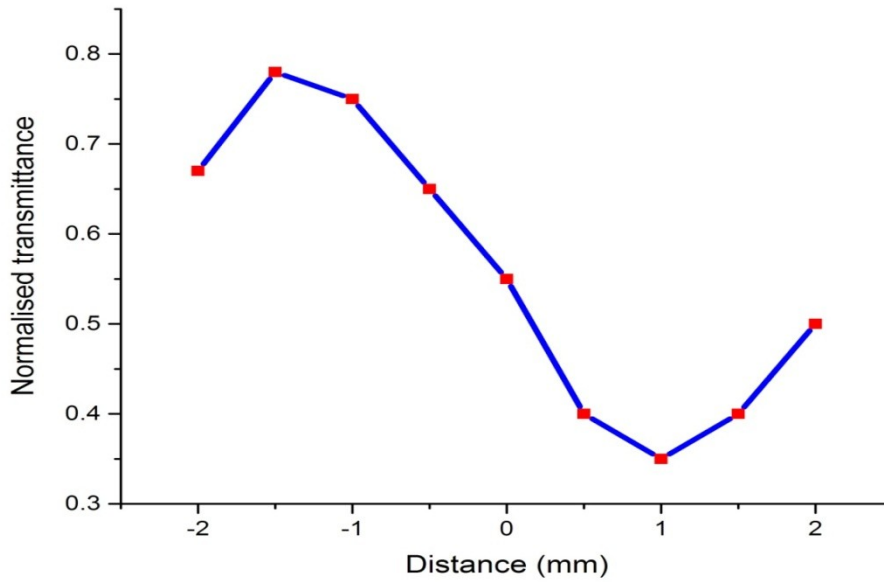| Crystals	The third order nonlinear optical susceptibility (χ3) (esu)	Reference
L-serine	11.04×10^{-8}	19
[Ag(L)2](NO3)·(MeOH)· (EtOH) (i) and [HgI2(L)] (ii) {L = 1,2-bis[(ferrocen-lylmethylene)amino]ethane}	i. 4.11×10^{-12} ii. 2.87×10^{-12}	20
Glycine potassium sulfate crystals	7.36×10^{-7}	21
Potassium dichromate single crystals	4.68×10^{-6}	22
SASM	**4.45×10^{-6}**	**Present work**

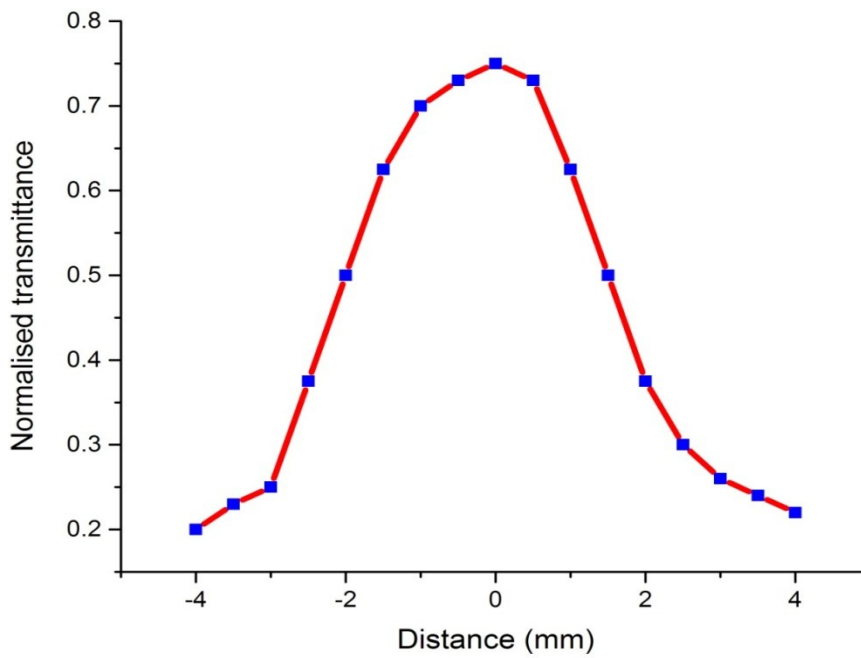**Fig. 7. Closed aperture curve of SASM crystal**

Fig. 8. Open aperture curve of SASM crystal

Conclusion

Single crystals of SASM have been successfully grown from an aqueous solution using slow evaporation technique. Single crystal and powder X-ray diffraction studies confirm the monoclinic crystal structure. UV-Vis-NIR spectrum reveals the UV cut-off wavelength at 278 nm. The vibrations of functional groups were identified by FTIR and FT-Raman spectra. The molecular structure of the grown crystal was established by ^{13}C-NMR spectroscopy. The second harmonic generation efficiency of SASM crystal was confirmed by green color emission. Third order nonlinear optical properties were determined and compared using Z-scan technique.

Acknowledgements

References

[1] D. S. Chemla, J. Zyss, Nonlinear Optical Properties of Organic Molecules and Crystals, Academic Press, New York (1987).

(2) P. N. Prasad, D. J. Williams, Introduction to Nonlinear Optical Effects in Molecules and Polymers, Wiley-Interscience, New York (1991).

(3) D. Xu, M. Jiang, Z. Tan, A new phase matchable nonlinear optical crystal L-arginine phosphate monohydrate, Acta. Chem. Sinica 41(1983) 570-573.

(4) M. Kitazawa, R. Higuchi, M. Takahashi, Ultraviolet generation at 266 nm in a novel organic nonlinear optical crystal: L-pyrrolidone-2-carboxylic acid, Appl. Phys. Lett. 64 (1994) 2477-2479.

[5] D. Kalaiselvi., R. Jayavel., Synthesis, growth and characterization of L-proline imercuricchloride single crystals for frequency conversion applications Appl. Phys. A-Mater., 107 (2012), 93.

[6] U. Charoen-In, P. Ramasamy, P. Manyum, Unidirectional growth, improved structural perfection and physical properties of a semi-organic nonlinear optical dichlorobis (L-proline)zinc(II) single crystal, J. Cryst. Growth, 362 (2013), 220-226.

[7] R. M. Kumar, D. R. Babu, D. Jayaraman, R. Jayavel, and K. Kitamura, Studies on the growth aspects of semi-organic l-alanine acetate: A promising NLO crystal, J. Crystal Growth, 275, (2005) 1935-1939.

[8] I. Cicili Ignatius, S. Rajathi, K. Kirubavathi and K. Selvaraju, Enhancement of second harmonic generation efficiency, laser damage threshold and optical properties of cobalt chloride doped with L-alanine single crystal, Journal of Nonlinear Optical Physics & Materials Vol. 25, No. 2 (2016) 1650017.

[9] Zi-Qiang Hu, Duan-Jun Xu and Yuan-Zhi Xu, (S)-Alanine-(S)-mandelic acid (1/1), Acta Cryst. E60 (2004) 269-271.

[10] M. Lydia Caroline, R. Sankar, R.M. Indirani, S. Vasudevan, Growth, optical, thermal and dielectric studies of an amino acid organic nonlinear optical material: L-alanine, Mat. Chem and Phy. 114 (2009) 490-494.

[11] M. Babij, A. Mondry, Synthesis, structure and spectroscopic studies of europium complex with S (+)-mandelic acid, Journal Of Rare Earths, 29 (2011) 1188-1191.

[12] P. Ilayabarathi, J. Chandrasekaran, Growth and characterization of l-alanine cadmium bromide a semiorganic nonlinear optical crystals, Spectrochim. Acta A 96 (2012) 684-689.

[13] Spectral database for organic compounds (SDBS), http://sdbs.db.aist.go.jp/sdbs/cgi-bin/direct_frame_top.cgi.

[14] M. L. Caroline, R. Sankar, R. M. Indirani and S. Vasudevan, Growth, optical, thermal and dielectric studies of an amino acid organic

nonlinear optical material: L-Alanine, Mater. Chem. Phys. **114** (2009) 490

[15] I. C. Ignatius, S. Rajathi, K. Kirubavathi and K. Selvaraju, Studies on growth and characterization of L-alanine strontium chloride trihydrate single crystals for optical applications, Optik **125** (2014) 4265.

[16] M. Malathi, S.L.Rayar, P.Selvarajan, Spectral Characterization, Dielectric, Mechanical and SHG Studies of Thiourea Doped L-Alanine Cadmium Chloride Crystals, IOSR Journal of Applied Physics (IOSR-JAP) e-ISSN: 2278-4861, PP 78-83.

[17] A. N. Vigneshwaran, P. Umarani, C. Ramachandra Raja, Studies on nonlinear optical ammonium pentaborate crystals, J Mater Sci: Mater Electron, DOI 10.1007/s10854-017-6938-y

[18] T. Thilak, M. Basheer Ahamed, G. Vinitha, Third order nonlinear optical properties of potassium dichromate single crystals by Z-scan technique, Optik 124 (2013) 4716– 4720.